11th INTERNATIONAL CONFERENCE ON CONTACT MECHANICS AND WEAR OF RAIL/WHEEL SYSTEMS (CM2018)
DELFT, THE NETHERLANDS, SEPTEMBER 24-27, 2018

TRACTION AND CURVING OF VEHICLES EQUIPPED WITH GUIDED INDEPENDENTLY ROTATING WHEELS

Andrea Bracciali, Gianluca Megna*

Dipartimento di Ingegneria Industriale, Università di Firenze, via Santa Marta 3, 50139 Firenze, Italy

* E-mail: gianluca.megna@unifi.it

Abstract: Modern advances in permanent magnet electric motors allow designing vehicles with gearless driven guided independently rotating wheels (GDGIRW). High precision controls allow to define simple and effective different strategies in straight track and in curves, such that the wheels belonging to the same "axle" are virtually coupled in straight track while torque control (with different angular speed) can be easily achieved in curves as train location in metros with ATO systems is constantly known. The paper discusses the advantages of a metro vehicle equipped with the GDGIRW architecture over a conventional architecture with bogies in terms of performances and track friendliness.

Keywords: Independently rotating wheels; driven guided IRW; motor wheels; traction; curving; adhesion; creep forces.

1. Introduction

Longitudinal and lateral creepages that inevitably arise during sharp curve negotiations of a vehicle equipped with bogies are responsible for rail gauge face wear and corrugation. Wheels, on their side, may show abnormally high flange wear and periodic out-of-roundness (polygonization). This is due to both the constraint of equal angular speed of the wheels of a wheelset and the necessity to keep the wheelsets parallel in order to run stably at the maximum speed.

The behaviour of a bogie is, as known from the literature [1, 2], strongly influenced by traction. A low primary yaw stiffness improves steering in coasting while it worsen the kinematic asset of the bogie (angle of attack, wheel-rail forces) during traction. Moreover, stability at high speeds in critical conditions (empty vehicle, worn wheel profiles, high adhesion) requires typically a high yaw stiffness.

This situation is the inevitable results of the never-ending conflict between guidance and stability that is intrinsic in all vehicles with rigid connection of the wheelsets to the carbody or to the bogie frame.

In this paper, the architecture of a vehicle with gearless driven guided independently rotating wheels (GDGIRW) is presented. Although Independently Rotating Wheels (IRW) are widely used in low-floor trams [3], to the authors' knowledge there are no application of self-propelled vehicles equipped with driven guided IRW. It will be shown that the proposed architecture, together with a simple and well-established philosophy of traction, may virtually eliminate lateral creep allowing the maximum traction in all situations.

A case study for a metro vehicle running through a very demanding section (track slope and curvature) is presented, comparing the results with a conventional metro vehicle.

The implications of the use of the adoption of GDGIRW technology are extremely relevant, impacting on carbody manufacturing, the number of doors per meter, the position of the auxiliary equipment as well as power electronics, HVAC and so on. This paper is focused on contact mechanics aspects, so modifications and advantages potentially introduced by the use of new concept vehicles using the DGIRW technology will be discusses in a future paper. It can be said that the vehicle architecture is modular and that has its perfect application in driverless metros where performances may be critical in steep and sharp curves situations.

2. The GDGIRW technology

Trying to prevent high lateral creep forces arising while negotiating sharp curves in all vehicles with conventional bogies, a number of self- or assisted-steering bogies were proposed in the past to reduce the angle-of-attack (AOA) of the wheelsets. Unfortunately, these techniques are not as widespread as one could expect. Bogies actively steered with actuators, known as "mechatronics bogies", suffer high costs and low reliability and maintainability, justifying the reluctance of system integrators and of final customers to embrace such solutions. Passively steered wheelsets / bogies had more success, but the various strategies (bracing, linking) introduce some degree of complication that is often not justified for conventional operations.

A way to remove longitudinal creep forces is the adoption of IRW technology. This is simply the way the wheels of any cart are connected to the vehicle structure, so this looks the natural choice also for railways. As longitudinal forces vanish, there are no stability problems and this led in the 1960's to several studies about the application of IRW to high speed trains to avoid hunting. When running

dynamics became better known they were readily abandoned.

In fact, the "differential effect" offered by the wheelset made of an axle and two rigidly connected tapered wheels ensures self-centring and, to some extent, also curving without the intervention of wheel flanges. Bogies equipped with IRWs, where the kinematic constraint of equal angular speed of the wheels is absent, are infamous for the absence of centring in straight track that leads to premature flange wear as one or more flanges within a bogie run in constant contact with the rail gauge face.

The Spanish company Talgo developed in the 1940's the Guided IRW (GIRW) architecture, which proved to be a successful application of IRW. It consists on a set of "triangular structures" supported by single – axis portal bogie (named *rodal* by the company) equipped with IRW. The *rodal* is driven by linkages connected to the carbodies and therefore runs centred, as it has no freedom around the vertical axis (Figure 1). One of the more interesting applications of the Talgo trains is the use of a passive tilting layout, where the secondary suspension is located above the centre of gravity of the carbody. This allows "Talgo Pendular" to run through curves at higher speeds offering the same comfort given by conventional slower trains.

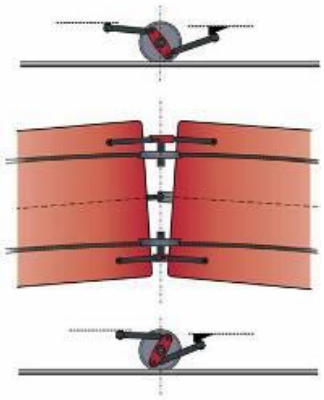

Figure 1 *Mechanism to steer IRW developed by the Spanish company Talgo.*

To the author's knowledge, Talgo manufactured trains made of conventional (with bogies) locomotives and hauled passenger cars equipped with *rodal*. Modern technology makes available driving chains that allow conceiving an architecture in which GIRW are driven, thereby adopting the concept of EMU (Electrical Multiple Unit) that is more and more widespread in railways and is the standard in metros since the application of electrification. The concept of gearless driven guided independently rotating wheels (GDGIRW) is therefore introduced in this paper.

3. Direct drive (gearless) motor wheels

Central to the technology of GDGIRW is the availability of electric motors that can be installed as close as possible to each wheel.

In recent years, the development of permanent magnet (PM) synchronous AC brushless motors for automotive application has been vertiginous. This kind of motors has a fixed hub (stator) with windings and a rotating part (rotor) equipped with permanent magnets. They were developed to drive electric and hybrid cars and are therefore "hidden" in the wheel web with a maximum external diameter of 17"-19" (Figure 2).

Figure 2 *In-wheel electric motors (left) and a motor wheel (right) for automotive applications.*

Typical performances offered by in-wheel motors for the automotive industry are far from the specifications of a modern metro vehicle, that require a typical specific power of 55÷60 kW/wheel and a starting torque of 3000 Nm/wheel. The greatest advantage in metro applications with web-mounted brake discs is that the motor does not have to fit in the wheel web, that the diameter can be increased and that the axial width is not strictly limited by the low-floor architecture of trams.

By applying the usual electric motor equations, it was estimated that a maximum starting torque of around 4500 Nm/wheel can be obtained. The direct coupling results in a gearless vehicle, so all gearbox maintenance operations are eliminated. Moreover, with PM brushless motors both speed and torque controls can be easily implemented as well as a precise position control down to stop. This means that electric braking is sufficient to stop and to hold the vehicles in all conditions and that the braking system is so lowly used that it can be downsized consistently. PM motors, in fact, guarantee dynamic braking when are not fed. In case of absence of power, the train comes to a stop automatically. A sketch of the volume occupied by a rotor supplying approximately 4500 Nm at the start is shown in Figure 3.

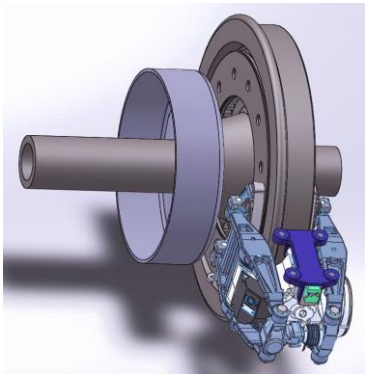

Figure 3 *Sketch of a wheel with a direct drive motor and a brake disc installed on the web. Starting estimated torque is 4500 Nm.*

4. Traction, curving and rail damage comparison of conventional and GDGIRW architectures in sharp curves

4.1. Vehicle description

In order to compare the behavior of conventional (A) and GDGIRW (B) vehicles, a simulation with the multibody code VI-Rail [4] was set up. The vehicles considered are typical of a metro application, and their characteristics are shown in Table 1. Although not many details can be provided here for space reasons, it can be seen that the vehicles have the same length and carry approximately the same number of passengers. The number of cars for the GDGIRW solution is clearly higher, resulting in smaller overthrows and therefore lower gauging problems. Loaded mass and lengths are slightly lower for the GDGIRW metro, resulting nevertheless in the same axleload. All the axles are driven, identifying this application as one to be used in very demanding operations in terms of resistance to motion.

Table 1 *Simulated vehicles.*

Vehicle name	A	B
Architecture	Conventional (bogies)	GDIGRW (*rodals*)
Number of cars	6	19
Car length	18 m	5.65 m
Number of bogies	12	N/A
Number of axles	24	20
Overall length	108 m	108 m
Total # of passengers	1208	1143
Axleload / wheel load	12 t / 6 t	12 t / 6 t
Number of driven axles	24	20
Fully loaded mass	288 t	240 t

In order to avoid misalignments of the end *rodals* of vehicle B, they were connected to the nearest *rodal* through a classical cross-bracing architecture. It should be remembered that this arrangement gives the desired results in constant radius curves, while in transitions the guidance may result not perfect. A sketch of the two vehicles is shown in Figure 4.

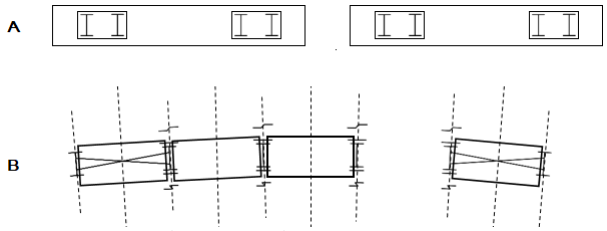

Figure 4 *Sketch of the layout of the conventional vehicle A (six cars) and of the DGIRW vehicle B (19 cars). End axles of vehicle B are guided by a classical cross-bracing mechanism driven by adjacent rodals.*

4.2. Adhesion considerations

An adhesion coefficient of f=0.4 was used to be consistent with all classical running dynamics conditions. It is nevertheless well known that in many case adhesion can be as high as f= 0.6, especially in dry, hot, long metro tunnels. The results shown in the following are therefore to be considered as conservative, in the sense that wear and tear will be amplified in more "sticky" conditions.

The full Kalker model implemented in the software package allows to define a saturation of the traction curve according to the maximum longitudinal creep until the adhesion force is passed. Simulations where conducted with a (piecewise defined) saturation curve that has a maximum of f=0.4 for a longitudinal creep γ_x=1.65% while it drops down to f=0.01 when the creep becomes γ_x=1.70%. This approximation tends to mimic the behavior of anti-spin systems installed in all normal vehicles. Traction control ramps up torque until the speed of all the axles is the same, leaving some room for the inevitable difference in the various wheels diameter. As an example, a locomotive tolerates a maximum difference on 25 mm in the diameter of nominal D=1100 mm, corresponding to a difference in speed of ±0.0116 = ± 1.16%. Speed differences larger than this are perceived by the control as spin or skid, interrupting traction or braking.

The simulations therefore resulted in a maximum torque for which the vehicle was not able to re-start once stopped. This is not fully true in the real life, as the traction control will try to exploit the full traction conditions again and again until the vehicle (hopefully) starts. A deeper description of traction controllers lays out of the scope of the present paper.

4.3. Simulated scenarios

As a general rule, *wear numbers* $W = T\gamma = T_x\gamma_x + T_y\gamma_y$ for both vehicles were calculated but only the results of the front bogie of vehicle A are shown, as the carbody-bogie frame torque is zero and the two bogies exhibit exactly the same behaviour. Selected profiles were S1002 for wheels and 60E1 laid 1:40 for rails to avoid double contact problems. For the sake of simplicity, the simulation of vehicle B was initially limited to a 5-cars symmetrical trainset.

As it is expected that the GDGIRW solution has no or little advantage vs. the conventional solution in flat straight track (see par. 5), a set of simulations were performed to investigate the differences in a "difficult" situation. The track chosen in all the following cases was therefore selected as a constant radius curve with R=200 m. This is nevertheless representative of a wide variety of situations that can be found in metros.

It is anticipated that a summary of the results obtained for both the front bogie of vehicle A (axles 1+2) and for the reduced formation of vehicle B (five cars, axles 1+2+3+4+5+6) is shown in Table 2. A graphical representation of the wear numbers limited to the front bogie of vehicle A is shown in Figure 5.

The AOAs for the first axle of both vehicle A and B are shown in Table 3, amply justifying the outcomes in terms of wear numbers.

The overall damage introduced in the rails by a full six-cars formation of vehicle A (24 axles) and by a full 19 cars formation of vehicle B (20 axles) is shown in Table 4. Beyond the wear number for specific wheels, this can well represent the advantage offered by the GDGIRW architecture.

Case # 1: starting in high-canted steep track
The track used for starting conditions has a slope of i=50‰ = 5% and a cant of h=160 mm (cant deficiency h_d=-160 mm). This track conditions can be found e.g. in ref. [5] and may be present in limited but significant line stretches worldwide.

The simulation was conducted starting with a small torque on a flat, straight track, then the vehicle started curving and climbing on a transition until it stopped in the steep, circular curve as the torque was insufficient to climb up the line. When the speed zeroed, a predetermined torque was applied *per axle*.

For vehicle A this results in different longitudinal (traction) forces depending on local contact conditions which are obviously different between the right and the left wheels, while for vehicle B (on which torque control is applied) the longitudinal forces are exactly the same as the wheels are independently driven.

The torque was increased stepwise until wheel slip was detected on vehicle A. This resulted in a maximum torque of 4500 Nm per axle (4500*24/288=375 Nm/t) and in an acceleration of 0.33 m/s^2.

The same torque was applied on each *rodal*, resulting in the same specific torque (4500*20/240=375 Nm/t). The fact that vehicle B has a lower resistance to motion leads to a slightly higher acceleration of 0.35 m/s^2.

Case # 2: starting in flat steep track
The same torques were applied in a similar scenario, i.e. starting on a track with the same slope of 50 ‰ but without cant.

In this case the damage introduced by vehicle B is negligible, while vehicle A exhibits wear number values similar to the canted case, confirming that cant is not related to damage in case of high cant excess.

Case # 3: coasting at 153 mm cant excess
The "natural" behavior of the two solutions was compared in coasting on canted track h=160 mm.

The simulation requested a programming trick to keep the vehicles running after one full circle. The software does not allow in fact to design tracks that intersect. The solution was found by designing a helical track with a helix pitch of –1 mm, resulting in a negligible artificial slope.

Starting speed in tangent track was set to 3.1 m/s as this is the speed that results in h_d=-153 mm (or a_{nc}=- 1 m/s^2 non-compensated acceleration). Vehicle A, due to slightly higher resistances during the approach, negotiated the circular curve at 2.5 m/s, with a negligible difference.

As the wheels rotate freely for vehicle B, no slip results in this direction and the damage is limited to the one given by lateral forces/creepages. Vehicle A keeps going on showing high wear number for the front wheelset, while the rear wheelset runs centered compensating for the track curvature introducing nearly no damage on the rails. Wear numbers are not negligible for vehicle A, and also vehicle B introduces minor damage in the rails.

Case # 4: coasting at balance speed
Increasing the initial speed to 14.5 m/s leads to balance in the curve (h_d=0, a_{nc}=0). As before, Vehicle A, due to slightly higher resistances during the approach, negotiated the circular curve at 14.38 m/s, with a negligible difference.

Regardless of the kinematic balance, wear numbers for vehicle A remain significant, while they vanish in practice for vehicle B.

Case # 5: coasting at 153 mm cant deficiency
Increasing further the initial speed to 20.3 m/s leads to h_d=+153 mm (or a_{nc}= + 1 m/s^2 non-compensated acceleration).

Due to the rotation of the bogie around the vertical axis given by centrifugal forces that are supported by the flange of the outer wheel of the first wheelset, wear numbers for vehicle A decrease with respect to the balance conditions. The same lateral forces generate more wear on vehicle B.

This case should be typical case for conventional railway lines with mixed traffic, in which freight trains negotiate curves run typically at a_{nc}= 0.6 m/s^2 while passenger trains run at a_{nc}= 1 m/s^2 on the same curves.

This is not the case for metros, for which the speed profiles is fixed (especially with ATO operation) and the tendency is to design cant in order to result in balance conditions that maximize passenger comfort. Anyway, also in this case, which is favourable for vehicle A and unfavourable for vehicle B, confirms that vehicle B is less damaging the low rail.

4.4. Comparison of vehicles A and B
Curving attitude is normally evaluated by considering the AOA of the wheelsets of the first bogie. Table 3 compares AOA the said axles of vehicle A to the first *rodal* of vehicle B.

It can be observed that AOA of the first wheelset of vehicle A are always larger than those of vehicle B, while the second wheelset of the vehicle A runs almost radially. This justifies the different wear numbers (Table 4).

The superiority of vehicle B on vehicle A in terms of rail damage is overwhelming. In the worst case vehicle B is less damaging of vehicle A by a factor 4, in the best case by a factor 400.

Table 2 *Wear numbers for the front bogie of vehicle A and for all the axles of a six cars train formation of vehicles B in the five simulated scenarios. Numbers in the cells are $T_x\gamma_x$ and $T_y\gamma_y$, while the bold values are the total wear number $T= T_x\gamma_x + T_y\gamma_y$.*

#	Type	v [m/s]	i [‰]	h [mm]	h_d [mm]		Vehicle A		Vehicle B					
							Axle 1	Axle 2	Axle 1	Axle 2	Axle 3	Axle 4	Axle 5	Axle 6
1	Traction	0	50	160	-160	Right	0/299 **299**	102/14 **116**	4/115 **119**	5/5 **10**	6/59 **65**	7/68 **75**	9/108 **117**	2/4 **6**
						Left	101/266 **368**	221/0 **221**	15/91 **106**	5/0 **5**	4/19 **23**	5/21 **26**	5/50 **55**	4/6 **10**
2	Traction	0	50	0	0	Right	2/209 **211**	257/1 **258**	3/1 **4**	4/0 **4**	2/0 **2**	4/3 **7**	3/0 **3**	3/0 **3**
						Left	104/362 **466**	55/1 **56**	3/0 **3**	3/0 **3**	2/0 **2**	3/0 **3**	2/0 **2**	3/0 **3**
3	Coasting	3.1	0	160	-153	Right	12/317 **329**	0/8 **8**	0/113 **113**	0/2 **2**	0/59 **59**	0/67 **67**	0/91 **91**	0/3 **3**
						Left	32/208 **240**	8/0 **8**	0/93 **93**	0/0 **0**	0/18 **18**	0/21 **21**	0/41 **41**	0/5 **5**
4	Coasting	14.5	0	160	0	Right	31/241 **272**	64/4 **68**	0/59 **59**	0/0 **0**	0/0 **0**	0/7 **7**	0/0 **0**	0/0 **0**
						Left	44/365 **409**	263/0 **263**	0/29 **29**	0/0 **0**	0/0 **0**	0/1 **1**	0/0 **0**	0/0 **0**
5	Coasting	20.3	0	160	+153	Right	100/260 **360**	100/260 **360**	0/101 **101**	0/0 **0**	0/9 **9**	0/9 **9**	0/57 **57**	0/7 **7**
						Left	25/430 **455**	42/3 **45**	0/121 **121**	0/120 **120**	0/38 **38**	0/40 **40**	0/133 **133**	0/6 **6**

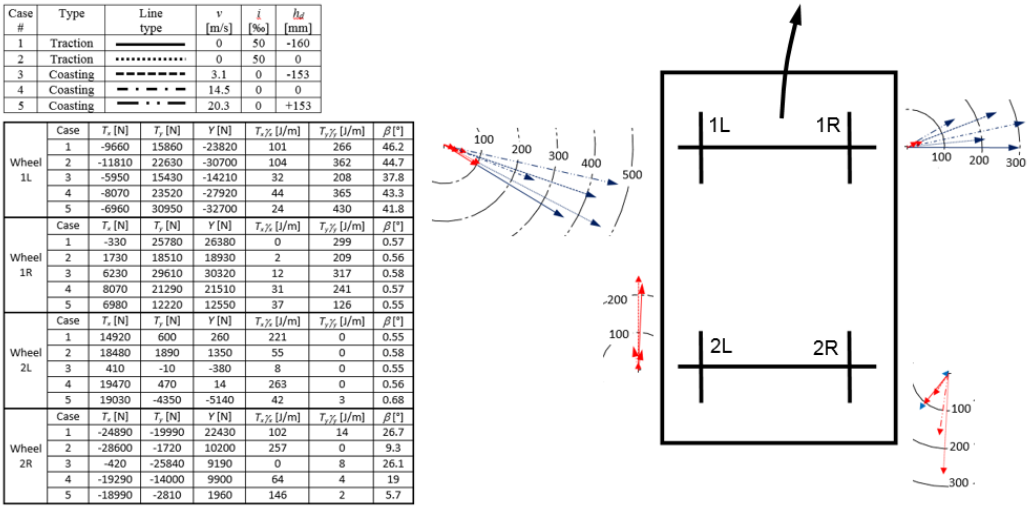

Case #	Type	Line type	v [m/s]	i [‰]	h_d [mm]
1	Traction	———	0	50	-160
2	Traction	·····	0	50	0
3	Coasting	– – – –	3.1	0	-153
4	Coasting	– · – · –	14.5	0	0
5	Coasting	— · · —	20.3	0	+153

	Case	T_x [N]	T_y [N]	Y [N]	$T_x\gamma_x$ [J/m]	$T_y\gamma_y$ [J/m]	β [°]
Wheel 1L	1	-9660	15860	-23820	101	266	46.2
	2	-11810	22630	-30700	104	362	44.7
	3	-5950	15430	-14210	32	208	37.8
	4	-8070	23520	-27920	44	365	43.3
	5	-6960	30950	-32700	24	430	41.8
Wheel 1R	1	-330	25780	26380	0	299	0.57
	2	1730	18510	18930	2	209	0.56
	3	6230	29610	30320	12	317	0.58
	4	8070	21290	21510	31	241	0.57
	5	6980	12220	12550	37	126	0.55
Wheel 2L	1	14920	600	260	221	0	0.55
	2	18480	1890	1350	55	0	0.58
	3	410	-10	-380	8	0	0.55
	4	19470	470	14	263	0	0.56
	5	19030	-4350	-5140	42	3	0.68
Wheel 2R	1	-24890	-19990	22430	102	14	26.7
	2	-28600	-1720	10200	257	0	9.3
	3	-420	-25840	9190	0	8	26.1
	4	-19290	-14000	9900	64	4	19
	5	-18990	-2810	1960	146	2	5.7

Figure 5 *Left: summary of longitudinal and lateral forces in the rail contact patch reference system, lateral forces in the global reference system, longitudinal and lateral wear numbers and wheel-rail contact angle for the front bogie of vehicle A in the five simulated scenarios. Right: plot of wear numbers. Vectors lay on the contact patch surface and point in the direction of the resulting force* $\boldsymbol{T}=T_x\,\boldsymbol{i} + T_y\,\boldsymbol{j}$*. Wear numbers are stacked, starting with $T_x\gamma_x$ (red) and ending with $T_y\gamma_y$ (dark blue). It can be observed that in most of the cases wear numbers are larger on the first wheelset, whose lateral forces are dominant on longitudinal forces. Note: lateral forces in the contact patch reference have no direct influence on lateral forces in the global reference system.*

Table 3 *Angle-of-attack (AOA) [mrad] for trainsets A and B running on a R=200 m right curve in different conditions*

#	Type	v [m/s]	i [‰]	h_d [mm]	Vehicle A first /second axle	Vehicle B first *rodal*
1	Traction	0	50	-160	11.7 / 0.8	4.48
2	Traction	0	50	0	11.4 / 0.4	0.21
3	Coasting	3.1	0	-153	11.3 / 0.3	-2.21
4	Coasting	14.5	0	0	10.6 / -0.3	4.25
5	Coasting	20.3	0	+153	10.3 / -0.7	-4.79

Table 4 *Wear numbers [J/m] for trainsets made of 6 cars (A) and 19 cars (B) running on a R=200 m right curve in different conditions*

#	Type	v [m/s]	i [‰]	h_d [mm]	Left/Right rail vehicle A	Left/Right rail vehicle B
1	Traction	0	50	-160	7200 / 4920	280 / 1250
2	Traction	0	50	0	6200 / 5400	80 / 80
3	Coasting	3.1	0	-153	3000 / 4000	400 / 1080
4	Coasting	14.5	0	0	8040 / 4000	20 / 100
5	Coasting	20.3	0	+153	6000 / 3730	1620 / 450

What is expected (and confirmed by the results) is the negligible damage introduced by vehicle B running in "near balance" conditions (i.e. cases 2 and 4). In the same cases vehicle A exhibits high wear numbers, that explain the extensive damages observed even if the vehicle runs in apparently favourable kinematic conditions.

Also in the cases of high cant excess (i.e. cases 1 and 3) vehicle B is superior. It can be concluded that the damage introduced in the rail by vehicle B is due only to traction forces at balance speed and that also in high-canted track wear numbers are relatively limited despite high gravitational forces.

Although rail damage is central in this paper, safety against derailment must be checked in all situations. It can be seen (Table 5) that vehicle B has derailment

coefficients *Y/Q* lower than vehicle A. In any case, estimated values are much lower than the maximum values allowed by running dynamics standard EN 14363 [6].

Table 5 *Y/Q derailment ratio for all the simulated cases*

#	Type	v [m/s]	i [‰]	h_d [mm]	Left/Right rail vehicle A front wheelset rear wheelset	Left/Right rail vehicle B first rodal
1	Traction	0	50	-160	0.53 / -0.41 -0.01 / -0.25	0.44 / -0.35
2	Traction	0	50	0	0.49/ -0.40 -0.02 / -0.14	0.02 / 0.00
3	Coasting	3.1	0	-153	0.44 / -0.38 0.00 / -0.14	0.25 / -0.20
4	Coasting	14.5	0	0	0.33 / -0.40 0.01 / -0.12	0.42 / -0.35
5	Coasting	20.3	0	+153	0.40 / -0.41 0.07 / -0.04	0.42 / -0.26

5. Rail damage in mild curves

As aforementioned, the convenience of the GDGIRW technology tends to vanish when the curvature of the line decreases, i.e. when the curves tend to become mild.

A large number of simulations was conducted with or without traction, slope, cant deficiency and so on. In the following the behavior of vehicles A and B is compared, for clarity, only during coasting with two levels of non-compensated acceleration (a_{nc}= 0 and a_{nc}= 1 m/s^2, corresponding to h_d=0 and h_d=153 mm), for five different curvatures (ρ=1/R=1, $\sqrt{2}$, 2, 3 and 5 km^{-1}) corresponding to R=1000, 707, 500, 333 and 200 m respectively.

The results are shown in Figure 6 for the balance speed case and in Figure 7 for the h_d=153 mm case.

As expected, the vehicle B with GDGIRW architecture introduces no damage at all in the rail at balance speed, while vehicle A seems to be not track friendly at all for R<400 m, a value typical for metros.

When cant deficiency increases, bogie rotation due to centrifugal effects makes vehicle A more friendly than in the balance case. In any case, the advantage offered by the adoption of the GDGIRW architecture is relevant or, at least, neutral.

To highlight the effect of traction, two simulations were conducted at v=22.9 m/s on an R=1000 m, h=80 mm curve (h_d=0) with and without the maximum torque of 4500 Nm per axle used above.

For vehicle A, the wear number for the front outer wheel raised from 71 J/m to 103 J/m passing from coasting to full traction. For vehicle B, wear numbers remained very low, changing from 1÷2 J/m to 3 J/m even with the maximum traction.

This has important consequences on rail damage in mild curves. Models developed by Burstow [7] and Öberg [8] identify the range of $T\gamma$ for which RCF damage is dominant over wear (Figure 8). It can be seen that vehicle A results in wear numbers in a range for which RCF damage is dominant, while vehicle B is constantly below the threshold of 15 J/m for which no damage is introduced in the rail. It results therefore that a conventional vehicle is able to damage the high rail regardless of the fact that it is coasting or in traction; on the opposite, vehicle B *never damages* the rail for any operating condition.

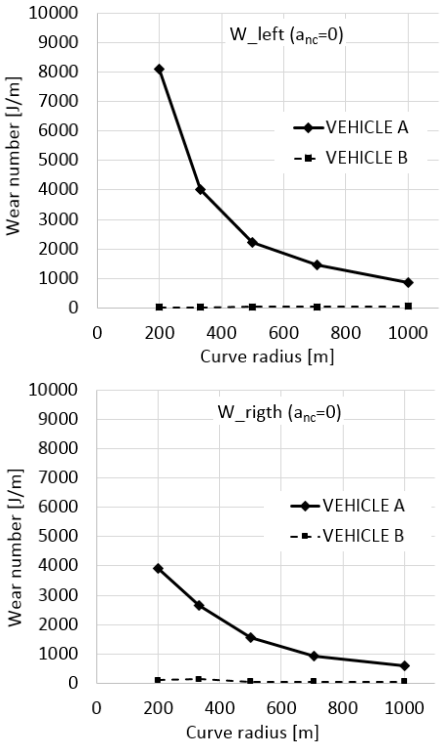

Figure 6 *Wear numbers [J/m] for trainsets made of 6 cars (A) and 19 cars (B) running at balance speed in curves of different radius.*

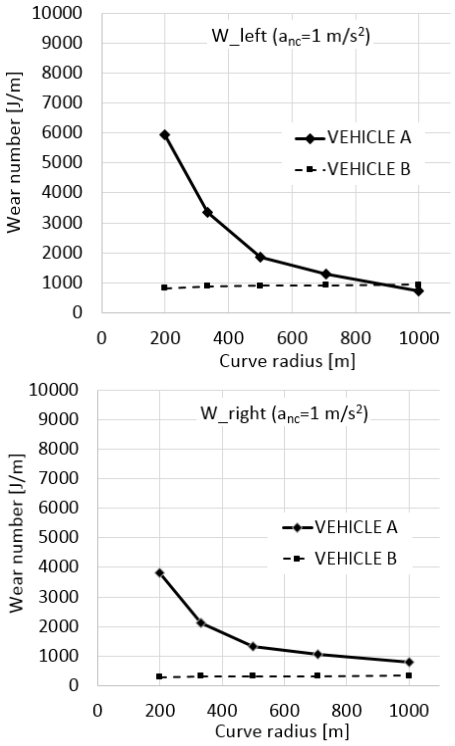

Figure 7 *Wear numbers [J/m] for trainsets made of 6 cars (A) and 19 cars (B) running at a_{nc}=1 m/s^2 (h_d=153 mm) in curves of different radius.*

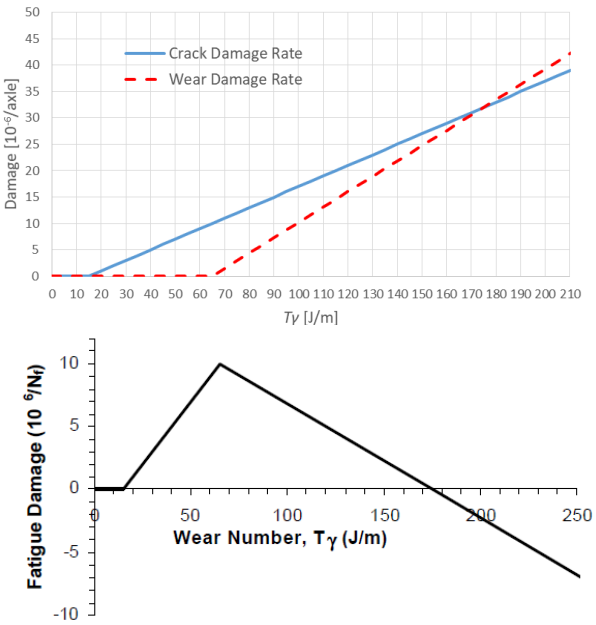

Figure 8 *Assumed damage rate for wear and crack growth as function of Tgamma in the Rail Surface Damage (RSD) model. After the break-even point at 175 J/m, wear is dominant on RCF and cracks are removed before they grow.*

6. Development of the GDGIRW technology

As already described, preliminary analyses show that permanent magnet (PM) "motor wheels" with a continuous torque of 3500 Nm and a starting torque of 4500 Nm can be designed in the larger spaces normally available for wheelsets compared to car wheels. Some problems are nevertheless foreseeable in the application of PM motors on GDGIRW vehicles.

First, service factors for a metro vehicle are particularly severe and a liquid cooling would probably be necessary. Compared to AC asynchronous motor, PM motors are known to be "cool" as there are no currents circulating in the rotor (equipped with permanent magnets) while the "hot" part of the motor is stationary (the stator) and can be cooled relatively efficiently.

Second, PM motors would work in a very hard conditions in terms of accelerations and shocks that are of a at least one order of magnitude higher than those experienced by motors mounted on cars equipped with rubber tyres.

It is not the intention of the authors to hide the technological problems linked to such new and promising technology, promoted by the vertiginous development of micro- and power electronics, but, once solved, it would offer distinct advantages as follows.

A further simulation was in fact performed with the best scenario of a starting torque of 4500 Nm *per wheel*, i.e. 9000 Nm per *rodal*. Conditions chosen for this analysis were the most critical ones already observed: starting on an i=5% slope in a curve with R=200 m and cant h=160 mm.

It is worth reminding that vehicle A started slipping at 4500 Nm *per axle*, with wear numbers as high as 7000 J/m on the high rail and 5000 J/m on the low rail.

Simulations on vehicle B led to an astonishing acceleration of 1.16 m/s^2 with wear numbers of 800 J/m of the high rail and 1390 J/m on the low rail. These figures show that the performances of a GDGIRW vehicles can be massively superior compared to a conventional vehicle. Moreover, to obtain the usual performances that are requested in purchasing tenders, the GDGIRW vehicle can be equipped with less than 100% of driven wheels saving consistent money and complications.

7. Conclusions

The distinct advantage of the GDGIRW architecture is the ability of aligning the "wheel axis" (the axle does not exist) always radially. These conditions eliminate virtually all creepages in a trailed *rodal*: longitudinal creepage is zero as wheels are freely rotating, while lateral creepage is zero as the *rodal* is guided by the carbodies and the angle of attack vanishes. The latter condition is obviously possible when the trainset runs in a constant radius curve, while during transitions the behaviour of the end axles must be properly managed.

With the GDGIRW layout, maximum accelerating and braking efforts can be obtained. Adhesion is partly "wasted" during negotiation of a conventional bogie due to longitudinal and lateral creepages. Both these phenomena dissipate energy and damage the surfaces in contact. This requires bigger motors installed on the vehicles and leads to undesired wheel and rail wear, tear and associated costs.

The paper has compared the behaviour of a conventional metro to that of a trainset built with the GDGIRW technology respecting the basic requirements in terms of axleload, number of passengers, acceleration, braking and so on. In particular, several scenarios to highlight the advantage that can be obtained in full and partial traction compared to conventional vehicles were simulated.

Although several complex control strategies are available for mechatronic bogies, the one used in this research is particularly simple and effective, consisting in a speed control in straight track and a torque control in curves managed, for example, by ATO system.

Wear numbers highlight that the damage introduced in the wheel-rail contact is minimum, avoiding lateral wear and longitudinal corrugation at the best. The GDGIRW architecture has the highest possible track friendliness and is virtually capable to avoid as well any damage due to Rolling Contact Fatigue.

The GDGIRW looks very promising in terms of both simplicity and performance once technological problems linked to cooling and vibrations are solved.

Acknowledgments

The authors acknowledge the help generously offered by Ms. Greta Urbani (University of Florence) and by Dr. Mauro Cavalletti (VI-Grade Italy).

References

[1] S.L. Grassie and J.A. Elkins: *Tractive effort, curving and surface damage of rails - Part 1. Forces exerted on the rails*, Wear, 2005, vol. 258, pp 1235–1244, doi:10.1016/j.wear.2004.03.064.

[2] S.L. Grassie and J.A. Elkins: *Traction and curving behaviour of a railway bogie*, Vehicle System Dynamics, 2006, vol. 44 Supplement, pp 883-891, doi: 10.1080/00423110600907451.

[3] A. Bracciali: *Railway wheelsets: history, research and developments*, International Journal of Railway Technology, 2016, vol. 5(1), pp 23-52, doi:10.4203/ijrt.5.1.2.

[4] Vi-Grade Engineering Software & Service, *Vi-Rail 18.0 Documentation*, Vi-Grade GmbH, Marburg, Germany, 2017.

[5] A. Bracciali: *Rail corrugation growth in a metro curve*, Proc. 7th International Conference on Contact Mechanics and Wear of Rail/Wheel Systems, Brisbane, Australia, September 24-27, 2006

[6] EN 14363:2016, *Railway applications - Testing and Simulation for the acceptance of running characteristics of railway vehicles - Running behaviour and stationary tests*, CEN, Brussels, 2016.

[7] M.C. Burstow: *A model to predict and understand Rolling Contact Fatigue in Wheels and Rails*, AEA Technology Rail, Derby, October 2003.

[8] J. Öberg and E. Andersson: *Determining Deterioration Cost for Railway Tracks*, Proc. IMechE Vol. 223, 2009, 121-129 Part F: J. Rail and Rapid Transit, doi:10.1243/09544097JRRT222